Transient Profiles in Ion-Exchange Displacement Chromatography

Shishir D. Gadam, Stuart R. Gallant, and Steven M. Cramer
Dept. of Chemical Engineering, Rensselaer Polytechnic Institute, Troy, NY 12180

A theoretical and experimental study of displacement development in cation-exchange displacement chromatography is carried out. Simulated displacement chromatograms are generated using a numerical model of displacement chromatography, which employs the steric mass action (SMA) formalism to describe the multicomponent nonlinear adsorption of proteins and polyelectrolytes. Simulated profiles of transient displacement chromatography are compared with experimental displacements over a range of operating conditions, and the model accurately predicts transient displacement behavior. The success of the model indicates that the SMA formalism is an appropriate tool for predicting multicomponent equilibrium adsorption of proteins. Simulated and experimental chromatograms indicate that significantly higher throughputs can be achieved by operating these protein displacement systems under nondeveloped conditions. In addition, displacement development proceeds faster at lower salt concentration, indicating that a reduction of the carrier salt concentration offers a means to further elevate the productivity of displacement systems. This work sets the stage for the optimization of protein displacement chromatography.

Introduction

Ion-exchange chromatography is ubiquitous in the downstream processing of biopharmaceuticals. Conventional overloaded elution mode, when employed for preparative chromatography, is often associated with significant peak tailing and dilution of the product (Knox and Pyper, 1986). Gradient mode, while overcoming dilution effects, requires sufficiently high separation factors in order to achieve the desired resolution. Displacement chromatography offers an alternative for preparative separations by overcoming disadvantages prevalent in both of the conventional operational modes (Horváth, 1985; Frenz and Horváth, 1988; Cramer and Subramanian, 1990). The displacement process is based on the competition of solutes for adsorption sites on the stationary phase according to their relative binding affinities and mobile phase concentrations. Displacement chromatography can maintain the inherent resolving power of linear elution chromatography while maintaining the high throughput and production concentration of gradient elution. These advantages of displacement chromatography make it particularly well suited for the downstream processing of biopharmaceuticals.

Correspondence concerning this article should be addressed to S. M. Cramer.

In the displacement mode, a packed bed is sequentially perfused with a carrier solution, a feed pulse, a displacer front, and finally a regenerant solution (Horváth, 1985; Frenz and Horváth, 1988; Cramer and Subramanian, 1990). The displacer is selected such that it has a higher affinity for the stationary phase than any of the feed components. The feed mixture to be separated is loaded under strongly retained conditions. The feed pulse is immediately followed by a constant infusion of the displacer compound in the carrier solution. The displacer drives the feed components ahead of the displacer front forcing strong competitive adsorption and facilitating separation. Under appropriate conditions, the action of the displacer causes the feed components to exit from the column as adjacent "square wave" zones of concentrated pure material in the order of increasing affinity of adsorption. Once the displacer front exits the column, an appropriate regeneration solution is passed through the column followed by reequilibration with the carrier.

The use of ion-exchange displacement chromatography for the purification of proteins has been investigated by a number of researchers (Peterson and Torres, 1983; Liao et al., 1987; Jen and Pinto, 1991; Gerstner and Cramer, 1992a,b;

Jayaraman et al., 1993; Gadam et al., 1993). Conventionally, displacement chromatography is carried out with feed loads small enough to ensure isotachic separations (full development). When the feed load is small, a fully developed train of adjacent square wave zones is achieved within the column. After this point, the displacement train travels through the rest of the column with no further separation. In order to maximize the column utilization in displacement chromatography, it is desirable to employ a column only as long as is required to furnish a complete separation of the product from the impurities. A number of studies have suggested that it is possible to increase the feed load beyond the maximum isotachic load while still achieving a complete separation (Liao et al., 1987; Ghose and Mattiasson, 1991; Gadam and Cramer, 1994). However, a rigorous comparison of simulated and experimental profiles in the displacement chromatography of proteins has not been reported to date. Such a study requires a model capable of representing the multicomponent adsorption of proteins in an environment of varying salt concentration.

Models of displacement chromatography may be divided into two categories: ideal and nonideal. In ideal models of chromatography, the mass transport effects are ignored resulting in a simpler, though quite often reasonably accurate, model. For ideal chromatography employing the multicomponent Langmuir isotherm, a transformation of variables known as the h- or ω-transform has been presented (Helfferich and Klein, 1970; Rhee et al., 1970). A number of authors have conducted theoretical or theoretical/experimental studies of ideal displacement chromatography using the multicomponent Langmuir isotherm (Frenz and Horváth, 1985; Rhee et al., 1989; Jen Pinto, 1992). Both Frenz and Horváth and Jen and Pinto have discussed the possibility of loading greater than isotachic feed loads in order to increase column productivity. Recently, some interesting work has been presented for ideal displacement chromatography governed by isotherms other than the multicomponent Langmuir (de Bokx et al., 1992).

When it is desirable to include mass-transfer resistances, these effects may be modeled in a number of ways (Helfferich and Carr, 1993). Generally, the solutions of the resulting systems of equations will require the use of a finite element or a finite difference technique. Nonideal displacement chromatography using the multicomponent Langmuir and other isotherms has been studied quite widely (Phillips et al., 1988; Gu et al., 1990; Antia and Horváth, 1991; Berninger et al., 1991; Yu et al., 1991; Felinger and Guiochon, 1993).

The multicomponent isotherm plays the crucial role in the calculation of displacement development (whether ideal *or* nonideal). To describe the equilibrium ion exchange of proteins, the steric mass action (SMA) formalism has been introduced (Brooks and Cramer, 1992; Gadam et al., 1993; Jayaraman et al., 1993). This model accounts for both the effect of salt on the adsorption of biomolecules and the effect of steric shielding, which occurs during the binding of large molecules to ion-exchange surfaces. Straightforward experimental protocols have been developed for independently determining the SMA model parameters (characteristic charge, equilibrium constant, and steric factor) of both proteins and high affinity displacers (Gadam et al., 1993; Gerstner and Cramer, 1992a,b; Jayaraman et al., 1993).

A simple analytical solution for the ideal displacement profile of an n-component mixture of proteins has already been presented and experimentally verified for fully developed (isotachic) separations (Brooks and Cramer, 1992; Jayaraman et al., 1993; Gerstner and Cramer, 1992a,b). Employing a column shorter than required for isotachic development will result in an "undeveloped" or "transient profile" emerging from the column. As might be expected, the calculation of a transient profile of an n-component mixture of proteins is somewhat more complex than an ideal isotachic profile. However, transient profiles are valuable for two reasons. First, in an isotachic separation, the bands are essentially pure; thus, the equilibrium within each band is that of the counterion and one protein with the stationary phase. In a transient profile, the proteins are still substantially mixed and equilibrium will be between the counterion and more than one protein. Thus, correct prediction of the transient profile represents a more demanding test of the reliability of the SMA formalism than prediction of the isotachic state.

Second, confirmation that SMA accurately predicts the length of column required for full separation lends insight into the optimization of displacement separations. It is, of course, desirable to employ a column only as long as is required to furnish a complete separation of the product from the impurities.

This article deals with a theoretical and experimental investigation of the transient behavior in cation-exchange displacement chromatography. The experiments have been selected both in order to test the SMA formalism's ability to predict multicomponent protein equilibrium and in order to investigate the development of displacement separations.

Theory

Equilibrium formalism

The SMA formalism is a three-parameter model of ion exchange designed specifically for representation of multicomponent protein-salt equilibrium adsorption. Development of SMA begins by assuming that the adsorption of a protein on the ion-exchange surface may be written in the form of a stoichiometric exchange with bound salt ions (Brooks and Cramer, 1992):

$$C_i + \nu_i \bar{Q}_1 \Leftrightarrow Q_i + \nu_i C_1 \tag{1}$$

where C_i and Q_i refer to the concentration of protein in the mobile phase and on the stationary phase, C_1 refers to the concentration of salt in the mobile phase, and $\bar{Q}_1$ refers to the concentration of bound salt available for exchange. The equilibrium constant of the reaction may be written as:

$$K_{1i} = \left(\frac{Q_i}{C_i}\right)\left(\frac{C_1}{\bar{Q}_1}\right)^{\nu_i} \tag{2}$$

The term "salt" is used generically throughout what follows; however, note that what is being discussed are monovalent cations (in cation-exchange chromatography) or anions (in anion-exchange chromatography). For example, in the simulations below, the proteins employed (α-chymotryp-

sinogen and cytochrome-C) have a positive characteristic charge as does the monovalent cation with which they are free to exchange: sodium.

Each protein molecule may sterically shield some salt counterions on the adsorptive surface. The quantity of salt counterions blocked by a particular protein will be proportional to the concentration of that protein on the surface:

$$\hat{Q}_{1i} = \sigma_i Q_i \tag{3}$$

Electroneutrality requires that:

$$\Lambda = \bar{Q}_1 + \sum_{i=2}^{NC} (\nu_i + \sigma_i) Q_i \tag{4}$$

Having introduced the SMA equations, a word about the meaning of the steric factor is necessary. In ion-exchange chromatography, nonidealities will be present in the mobile and stationary phases. Of course, these nonidealities may be accounted for by use of activity coefficients. However, since one of the dominant sources of nonideality is the differences in relative size of the adsorbed components, as suggested originally by Velayudhan, it is reasonable to modify the model to include this effect explicitly (Velayudhan, 1990). Myers has discussed explicit inclusion of nonideal effects in order to avoid the need for activity coefficients in adsorption on activated carbon (Myers, 1983). Thus, the steric factor may be looked upon as a lumped parameter that includes a number of mobile and stationary phase nonidealities of which the dominant nonideality is expected to be steric shielding.

Mass transport equations

The model employed to describe mass transport in this work is a single parameter, lumped dispersion model (Czok and Guiochon, 1990; Ma and Guiochon, 1991). Equation 5 describes transport in the packed bed of a chromatography column:

$$-D_i \frac{\partial^2 C_i}{\partial Z^2} + u_0 \frac{\partial C_i}{\partial Z} + \frac{\partial C_i}{\partial t} + \frac{1-\epsilon}{\epsilon} \frac{\partial Q_i}{\partial t} = 0 \tag{5}$$

where Z is axial position, t is time, ϵ is the total porosity of the column, u_0 is related to the superficial velocity by $u_0 = u_s/\epsilon$, and D_i represents an effective dispersion coefficient. The stationary phase is assumed to be in local equilibrium with the mobile phase

$$Q_i = F_i(C_1, C_2, \ldots C_{NC}) \tag{6}$$

where the equilibrium expression F_i is the SMA formalism discussed above. Because the mass transport equations include this local equilibrium assumption, the use of this type of model is restricted to relatively small stationary phase particles such as those employed in this study. In order to model the impact of mass transport resistance between the mobile and stationary phase, a more extensive mass transport model could be employed (Phillips et al., 1988; Gu et al., 1990; Berninger et al., 1991; Yu et al., 1991). For the purposes of this study, the more abbreviated model was utilized in order to reduce the time required for model solution.

To define a solution, appropriate initial and boundary conditions must be supplied. The initial conditions are

$$\begin{aligned} C_1(0,Z) &= C_{1,f} \\ C_i(0,Z) &= 0 \qquad i \neq 1 \\ Q_1(0,Z) &= \Lambda \\ Q_i(0,Z) &= 0 \qquad i \neq 1 \end{aligned}$$

where $C_{1,f}$ represents the carrier sodium concentration at the inlet of the column. During operation, the counterion concentration at the inlet of the column is held constant:

$$C_1(t,0) = C_{1,f}$$

After equilibration, the column is loaded

$$C_i(0 < t < t_f, 0) = C_{i,f}$$

$$C_{NC}(0 < t < t_f, 0) = 0$$

where component NC is the displacer and t_f is the length of the feed pulse. Subsequently, displacement occurs:

$$C_i(t > t_f, 0) = 0$$

$$C_{NC}(t > t_f, 0) = C_{NC,f}$$

Solution of model equations

To solve this system of partial differential equations, a numerical technique developed by Guiochon and coworkers was employed (Czok and Guiochon, 1990; Ma and Guiochon, 1991). In this technique, the system of partial differential equations describing ideal chromatography is solved by a finite difference method:

$$g_i^n = g_i^{n-1} - \frac{\Delta\tau}{\Delta z}(c_i^{n-1} - c_{i-1}^{n-1}) \tag{7}$$

where $g = c + \phi q$, c and q represent nondimensionalized mobile and stationary phase concentrations, ϕ represents a nondimensionalized phase ratio, τ and z represent nondimensional time and length coordinates, and n and i represent time and spatial indices. Note that Eq. 7 is merely a finite difference form of Eq. 5 from which the dispersion term has been deleted.

Equation 7 is a finite difference approximation of the transport equation of ideal chromatography. Since Eq. 7 is a first-order Taylor series approximation of the true solution, some error is associated with this calculation. Fortunately, this error may be employed to advantage. The error, termed "numerical dissipation," has the property that it causes steep concentration gradients or shocks within the solution to become more diffuse. Guiochon and coworkers have shown that this numerical dissipation may be employed to approximate the actual dispersion that occurs in a chromatography column (Czok and Guiochon, 1990; Ma and Guiochon, 1991).

Thus, Eq. 7 may be employed to provide an approximate solution to Eq. 5.

Simple relations exist between the observed efficiency of the chromatography column, the effective dispersion of Eq. 5, and the dimensions of the finite difference grid (Czok and Guiochon, 1990; Ma and Guiochon, 1991):

$$\frac{H}{L} = \frac{2D_i}{Lu_0} = \Delta z - \frac{1}{1+k'}\Delta\tau \tag{8}$$

where H is the height equivalent to a theoretical plate, L is the column length, and k' is the capacity factor in linear chromatography.

In ion-exchange chromatography, the fastest component in the column will be one that is unretained and moves at nondimensional velocity one. Thus, the stability of the finite difference method requires that:

$$\frac{\Delta\tau}{\Delta z} \le 1 \tag{9}$$

The model described above is employed throughout this article to simulate the transient behavior of protein displacement systems under a range of conditions. Simulated chromatograms were generated with a computer program written in FORTRAN. The program was run on an IBM ES/9000 Model 580 mainframe computer using IBM VS FORTRAN under the MTS operating system. During the course of each computer simulation, approximately two CPU minutes elapsed.

Simulation of the displacer front

Examination of Table 1 reveals that the displacer's equilibrium constant (5.5×10^{44}) and its characteristic charge (64) are substantially larger than the corresponding protein parameters. Given the fact that the displacer is a linear polyelectrolyte with a high charge to mass ratio, these parameters are not surprising; however, they do present a problem for simulation. The parameters themselves were estimated using the procedures described by Gadam et al. (1993) with Microsoft's Excel program, which is capable of representing quantities well in excess of 1.0×10^{100}. Unfortunately, the displacer equilibrium constant is larger than the maximum representable number within IBM VS FORTRAN.

In order to simulate the displacer, the affinity theory of Brooks and Cramer was employed (Brooks and Cramer, 1994). This theory represents a convenient tool for scaling the adsorption parameters of the displacer. The scaling produces a set of parameters: $K_{1,d,\text{pseudo}}$, $\sigma_{d,\text{pseudo}}$, and $\sigma_{d,\text{pseudo}}$. These pseudo-displacer parameters may be employed to simulate a front that has the same *breakthrough time* and *induced salt gradient* as the original unscaled front. Further, according to the theory, the scaled front will have the same *affinity*, that is, the same ability to displace proteins. The theory states that any displacer that has the same affinity parameter λ_i will have the same displacer efficacy:

$$\lambda_i = \sqrt[\nu_i]{\frac{K_{1i}}{\Delta}} \tag{10}$$

where $\Delta = Q_d/C_d$ is the partition coefficient of the displacer. Using this theory, a pseudo displacer was developed with the following properties: characteristic charge of one ($\nu_{d,\text{pseudo}} = 1.0$); steric factor reduced by the same factor ($\sigma_{d,\text{pseudo}} = \sigma_{d,\text{original}}/\nu_{d,\text{original}} = 2.17$); and concentration enlarged by the same factor ($C_{d,\text{pseudo}} = C_{d,\text{original}}{}^{*}\nu_{d,\text{original}}$). Finally, the pseudo-displacer equilibrium constant was chosen using the following iteration function:

$$K_{1,d,\text{pseudo}} = \Delta^{1-\frac{1}{\nu_{d,\text{original}}}} 10^{\frac{\log(K_{1,d\text{original}})}{\nu_{d,\text{original}}}} \tag{11}$$

$$0 = \Delta - K_{1,d,\text{pseudo}}\frac{\Lambda - (\nu_{d,\text{pseudo}} + \sigma_{d,\text{pseudo}})\Delta C_{d,\text{pseudo}}}{C_1} \tag{12}$$

where $\Delta = Q_{d,\text{original}}/C_{d,\text{original}} = Q_{d,\text{pseudo}}/C_{d,\text{pseudo}}$ is the iteration variable. The use of these pseudo-displacer parameters allows simulations employing high-affinity displacers such as 40 kD DEAE dextran to proceed without numerical overflow. For presentation in the figures, the displacer front was scaled back using the transformation: $C_{d,\text{original}} = C_{d,\text{pseudo}}/\nu_{d,\text{original}}$.

Table 1. Equilibrium and Transport Parameters Employed in Simulation

Column Capacity (Λ):	590 mM		
Plates/Meter at $k' = 2(N)$:	3,500 m^{-1}		
Void Fraction (ϵ):	0.70		
Solute	Charact. Charge (ν_i)	Steric Factor (σ_i)	Equilib. Const. (K_{1i})
Sodium	1.0	9	1.0
α-Chymotrypsinogen	5.0	44	5.5×10^{-3}
Cytochrome-C	5.9	54	6.9×10^{-3}
40 kd DEAE dextran	64	138	5.5×10^{44}

Experimental Methods

Materials

Strong cation exchange (sulfopropyl, 8 μm, 100×5 mm ID) columns were donated by Millipore (Waters Chromatography Div., Millipore, Milford, MA). Sodium monobasic phosphate, sodium dibasic phosphate, α-chymotrypsinogen, and cytochrome-C were purchased from Sigma Chemical Co. (St. Louis, MO). The displacer, 40 kD DEAE dextran, was donated by Pharmacia-LKB Biotechnology (Uppsala, Sweden). 10-kD molecular weight cut-off cellulose triacetate membranes were obtained from Sartorius (Goettingen, Germany). Polyvinylsulfuric acid potassium salt (PVSK), polydiallyl dimethyl ammonium chloride (polyDADMAC) and indicator *o*-toluidine blue were obtained from Nalco Chemical Co. (Naperville, IL).

Apparatus

Diafiltration of the 40 kD DEAE dextran displacer was carried out in an Amicon 8050 stirred cell (Amicon, Danvers, MA) using the cellulose triacetate UF membranes. All displacement experiments were carried out using a Model LC

2150 pump (LKB-Produkter AB, Bromma, Sweden) connected to the chromatographic columns via a Model C10W 10-port valve (Valco, Houston, TX). Fractions of the column effluent were collected using LKB 2212 Helirac fraction collector (LKB-Produkter AB, Bromma, Sweden).

Protein analysis of the collected fractions was carried out using a Model Waters 590 HPLC pump (Waters, Millipore, Milford, MA), a Model 7125 sampling valve (Rheodyne, Cotati, CA), a spectroflow 757 UV-VIS absorbance detector (Applied Biosystems Ltd., Foster City, CA) and a Model C-R3A Chromatopac integrator (Shimadzu, Kyoto, Japan). Sodium analysis was done using a Perkin-Elmer, Model 3030 (Perkin-Elmer, Norwalk, CT) atomic absorption spectrophotometer. Lyophilization was carried out using a Model Lyph Lock 4.5 Freeze Dry System (Labconco, Kansas City, MO).

Procedures

Estimation of Model Parameters. The adsorption parameters and transport parameters of the proteins are listed in Table 1. These parameters were determined on strong cation exchange columns (sulfopropyl, 8 μm, 100×5 mm I.D.) using the experimental procedures described by Gadam et al. (1993). [Note that the values in Table 1 differ slightly from previously reported values (Gadam, 1993) since different lots of protein and stationary phase were employed in this study.] The carrier was buffered using a combination of sodium monobasic and dibasic phosphate, the ratio chosen to give the appropriate pH range. The desired concentration of sodium ions was obtained subsequently by addition of sodium chloride. The final pH was adjusted using phosphoric acid.

At a flow rate of 0.1 mL/min, the efficiency of the column was determined by measuring the width at half-height of separate dilute injections of α-chymotrypsinogen and cytochrome-C; an average of the resulting efficiencies was employed.

Purification of DEAE Dextran. DEAE dextran (40 kD) was diafiltered using a 10 kD molecular weight cut-off membrane to remove salts and other low molecular weight impurities. After diafiltration, the retentate was lyophilized.

Operation of the Displacement Chromatograph. In all displacement experiments, the columns were initially equilibrated with the carrier and then sequentially perfused with feed, displacer, and regenerant solutions. The feed and the displacer solutions were prepared in the same buffer as the carrier. Fractions of the column effluent were collected directly from the column outlet to avoid extracolumn dispersion of the purified components.

Displacement Chromatography of Proteins in Cation Exchange Systems. Feed mixtures of α-chymotrypsinogen and cytochrome-C were separated by displacement chromatography using DEAE-dextran displacer in a strong cation exchange (SCX) column. The operating conditions are given in the figure legends of the corresponding displacement chromatograms and in Table 2. All displacement experiments were carried out at room temperature at a flow rate of 0.1 mL/min using a carrier, pH 6.0, buffered with sodium phosphate. Fractions of 100 μL were collected for subsequent analysis of protein and displacer.

Regeneration. The column was regenerated after each displacement experiment by passing ten column volumes of a 1-M NaCl solution in 100 mM phosphate buffer, pH 11.0.

Table 2. Conditions for Displacement Experiments

Mobile phase:	Sodium phosphate; pH: 6.0
Column:	100×5 mm I.D. Waters SP8HR
Flow Rate:	0.1 mL/min
Column Dead Volume:	1.37 mL

Fig.	Feed Vol. mL	Feed Vol. V_0	α-Chy Conc. mM	Cyt C Conc. mM	Displacer Conc. mM	Sodium Conc. mM
1a	0.96	0.70	0.48	0.87	0.75	75
1b, 2	1.37	1.00	0.45	0.86	0.75	75
1c, 3	2.40	1.75	0.45	0.86	0.75	75
1d, 4	5.10	3.72	0.48	0.88	0.75	75
5	3.50	2.55	0.44	0.83	0.78	20
6	2.40	1.75	0.48	0.86	0.75	97

Protein Analysis by HPLC. Protein analyses of the fractions collected during the displacement experiments were performed by ion-exchange HPLC under isocratic elution conditions. Sodium phosphate, 160 mM at pH 6.0, was employed as mobile phase in a strong cation exchange column. Displacement fractions were diluted 10–100 fold with the eluent and 20-μL samples were injected at a flow rate of 0.5 mL/min. The column effluent was monitored at 280 nm.

Displacer Analysis. 40 kD DEAE dextran displacer was analyzed using a colloidal titration assay provided by Nalco Chemical Company. 25 μL of the displacer solution in 50 mL deionized water background was titrated against PVSK reagent using *o*-toluidine indicator. Linear calibrations were generated using appropriate standards.

Results and Discussion

The transient behavior in ion-exchange displacement systems is important for two reasons. First, the optimum throughput in displacement systems often does not occur under isotachic operating conditions. Second, the application of the chromatographic model to predict transient profiles during displacement represents a demanding test of the ability of the SMA formalism to predict multicomponent equilibrium in ion-exchange systems. In the past, SMA-based models have been employed to describe the behavior of isotachic displacement separations in anion- and cation-exchange chromatography (Jayaraman et al., 1993; Gerstner and Cramer, 1993). In this article, transient displacement behavior is investigated using experiments in concert with a numerical model of displacement chromatography that employs the steric mass action (SMA) equilibrium formalism.

Effect of increasing the feed load on displacement separation

The proteins and displacer used in this study were α-chymotrypsinogen, cytochrome-C, and 40 kD DEAE-dextran. The nonlinear adsorption behavior of these solutes and isotachic displacement separation of these proteins have been examined previously (Gadam et al., 1993; Jayaraman et al., 1993).

Various stages of nondevelopment were generated by systematically increasing the feed volume in a series of four displacement experiments. (The comparison of simulations and experiment will be presented later in the article.) Experimen-

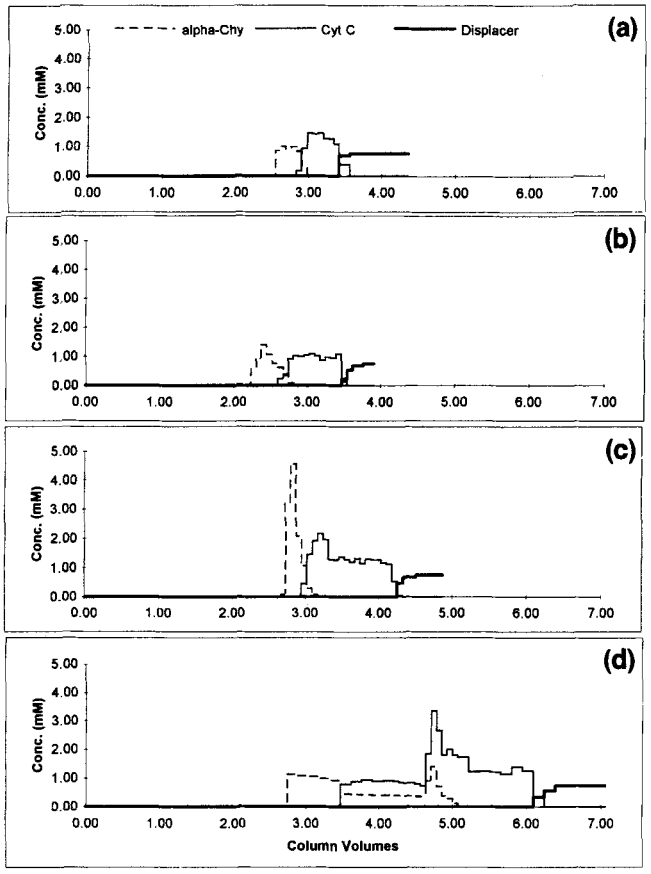

Figure 1. Displacement chromatograms of the proteins α-chymotrypsinogen (α-chy) and cytochrome C (cyt C) in a mobile phase of 75-mM sodium phosphate at pH: 6.0 displaced by 0.75-mM 40 kD DEAE dextran.

The concentrations and feed volumes of the proteins are: (a) 0.48-mM α-chy, 0.87-mM cyt C in 0.70 column volumes; (b) 0.45-mM α-chy, 0.86-mM cyt C in 1.00 column volumes; (c) 0.45-mM α-chy, 0.86-mM cyt C in 1.75 column volumes; (d) 0.48-mM α-chy, 0.88-mM cyt C in 3.72 column volumes.

tal conditions employed in these displacements are presented in Table 2. In the first series of experiments, the mobile phase salt concentration at the inlet to the column was 75 mM, and the displacer concentration was 0.75 mM. The proteins were loaded at concentrations of 0.48-mM (11.5-mg/mL) α-chymotrypsinogen and 0.87-mM (10.8-mg/mL) cytochrome C. Using the SMA-based chromatographic model, it was predicted that the separation of a feed volume of 0.96 mL (a total of 21.4 mg of protein loaded in 0.7 column volumes) constituted the maximum possible feed volume that would allow isotachic development. As seen in Figure 1a, a classical isotachic displacement separation of the two components is achieved.

Figure 1a and the succeeding chromatograms are presented using "column volumes" (or "column dead volumes") as the abscissa unit. An unsorbed molecule will emerge from the column at 1 column volume, measured at 1.37 mL using a tracer capable of exploring the pore space of the column employed in these experiments. (No measurable size exclusion effects were observed with any of the proteins or displacers employed in this study.)

To put this loading in perspective, *single component binding capacities* (that is, the amount of a protein that would be bound by the entire column in single component frontal operation under the given conditions) were calculated using the SMA formalism and the parameters listed in Table 1. At 75 mM salt concentration, passing a front of 0.48-mM α-chymotrypsinogen would result in binding of 71.2 mg of protein to the column. The α-chymotrypsinogen loaded in the experiment shown in Figure 1a corresponds to 16% of the single component binding capacity of the column for that protein. At 75-mM salt concentration, passing a front of 0.87-mM cytochrome C would result in the binding of 42.2 mg of protein to the column. The cytochrome C loaded in the experiment shown in Figure 1a corresponds to 25% of the single component binding capacity of the column for cytochrome C. Thus, considering the column capacity at 75 mM salt, a substantial amount of protein has been loaded in the isotachic experiment.

Figure 1b shows the separation of the same two proteins with the feed volume increased to one column volume (1.37 mL), all other conditions remaining the same as in Figure 1a. As seen in the Figure 1c, the first component, α-chymotrypsinogen, has formed a partially developed band while the cytochrome C has formed an isotachic square band. Because development proceeds from the rear of the displacement train to the front, it is to be expected that an increase in the feed volume would affect the front of the displacement train first.

The feed volume was further increased to 1.75 column volumes (2.4 mL), all other conditions remaining the same. This feed volume represents approximately 2.5 times that of the isotachic feed load employed in Figure 1a. As seen in the figure, this experiment resulted in a partial nondevelopment of cytochrome C and complete nondevelopment of α-chymotrypsinogen. The striking feature of this experiment is that, in spite of the high loading (36% of the single component binding capacity for α-chymotrypsinogen and 61% of the single component binding capacity for cytochrome C), an almost complete separation of the two components is achieved on the same column length. Clearly, it is important to be able to simulate these transient displacement systems in order to facilitate the determination of optimum conditions for maximum productivity.

Finally, a feed volume of 3.72 column volumes (5.1 mL) was employed (Figure 1d). In this experiment, the feed loading continued after the proteins had saturated the column. This experiment was carried out to generate a complex combination of multicomponent frontal and nondeveloped displacement chromatography. Clearly, the goal of this experiment was not to achieve a separation, but rather to generate an extremely difficult challenge to the chromatographic model because of the extensive mixed regions in the final chromatogram.

Comparison of experimental and simulated transient profiles (75-mM salt)

Experimental results presented above suggest that for a given column length, the feed load can be increased significantly beyond the isotachic feed load without loss of separation. Clearly, it is desirable to employ the maximum possible feed load and retain complete separation on a given column.

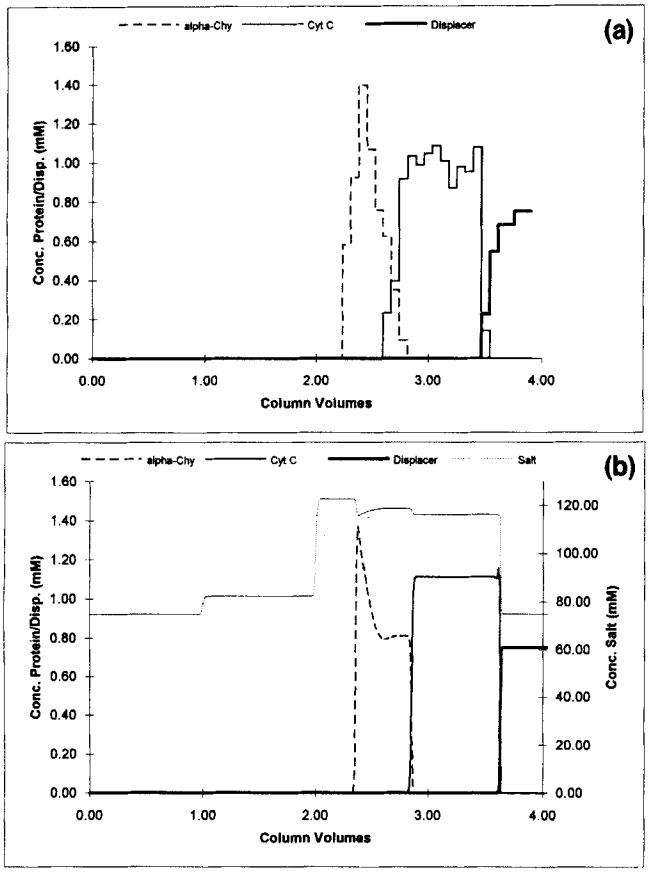

Figure 2. Transient displacement of α-chymotrypsinogen and cytochrome C by 0.75-mM 40 kD DEAE dextran in 75-mM sodium phosphate at pH: 6.0.

(a) Separation of 0.45-mM α-chy, 0.86-mM cyt C in 1.00 column volumes; (b) simulation.

In previous work, the SMA equilibrium formalism in conjunction with appropriate mass balance equations has been shown to accurately model both isotachic displacement trains and induced salt gradients (Brooks and Cramer, 1992; Jayaraman et al., 1993; Gerstner and Cramer, 1992a,b). The following discussion will focus on the comparison of the chromatographic model simulations with the transient displacement experiments. The model equations and the techniques of parameter estimation were discussed above. The model parameters are presented in Table 1.

At the outset of this discussion, it is important to mention the method of fraction collection and analysis. During each experiment, 100 μL fractions of the column effluent were collected, and each fraction was analyzed off-line. As a result, the experimental chromatograms have a discontinuous contour. In contrast, the simulated chromatograms have a smooth contour in order to provide the maximum amount of information about these transient displacement systems. The effect of fraction collection will be examined in more detail in the discussion related to Figure 5.

Figures 2a and 2b present a comparison of simulated and experimental displacements for the conditions described for Figure 1b. The feed load is 1.4 times the maximum isotachic feed load. Examining the simulated chromatogram (Figure 2b) from right to left, the displacer has broken through at the expected point (approximately 3.6 column volumes), and the cytochrome C emerges as a square band at approximately 1.1 mM concentration. Although the nondevelopment of the α-chymotrypsinogen is slightly more pronounced in the experiment than in the simulation, nondevelopment can clearly be seen in both figures.

Figures 3a and 3b present a comparison of simulated and experimental displacements for the conditions described for Figure 1c. The feed load is 2.5 times the maximum isotachic feed load. As seen in the figures, the model simulation is in good agreement with the nondeveloped displacement experiment. Again, the displacer breakthrough is well predicted (approximately 4.3 column volumes). In the simulated displacement (Figure 3b), the cytochrome C zone has formed a substantial square zone at the rear of the train with a concentration of approximately 1.1 mM. Toward the beginning of the cytochrome C zone, a region of nondevelopment has caused a spike in concentration. A small mixed zone exists at the interface between the cytochrome C and α-chymotrypsinogen bands. The elution volume of this mixed region is well simulated (at approximately 3 column volumes). Finally, a pure spike of underdeveloped α-chymotrypsinogen emerges at a concentration of 5 mM at the start of the displacement

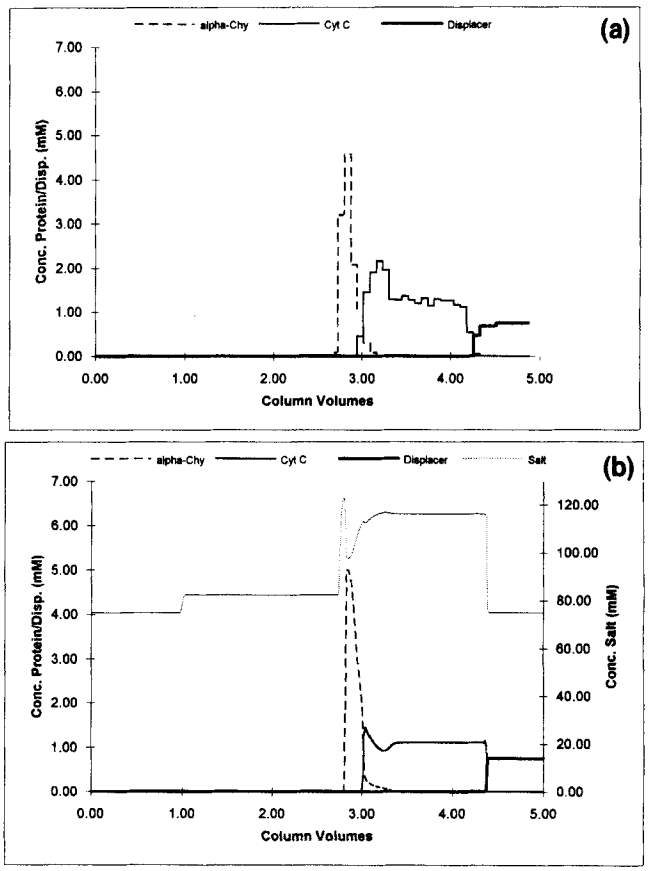

Figure 3. Transient displacement of α-chymotrypsinogen and cytochrome C by 0.75-mM 40 kD DEAE dextran in 75-mM sodium phosphate at pH: 6.0.

(a) Separation of 0.45-mM α-chy, 0.86-mM cyt C in 1.75 column volumes; (b) simulation.

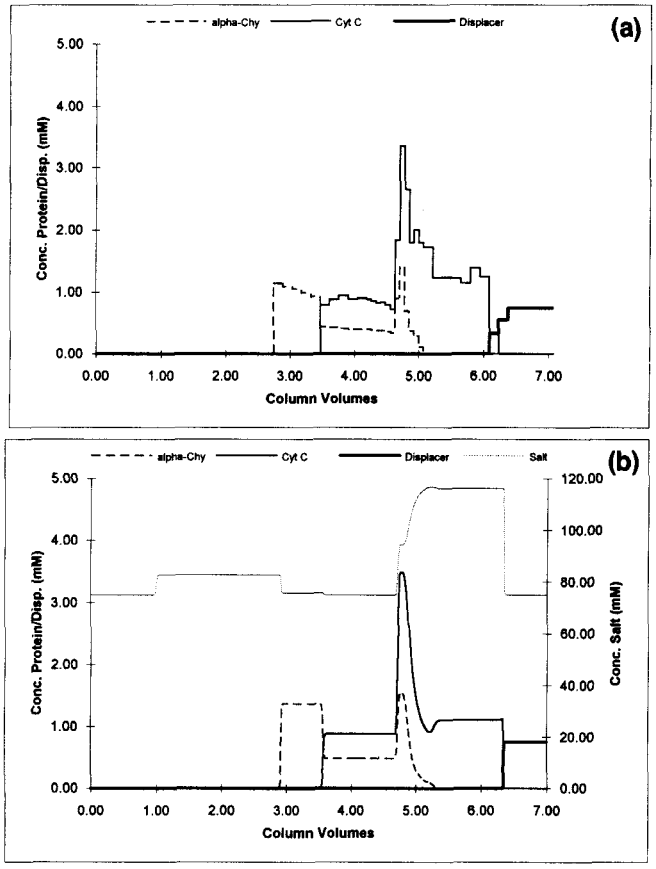

Figure 4. Transient displacement of α-chymotrypsinogen and cytochrome C by 0.75-mM 40 kD DEAE dextran in 75-mM sodium phosphate at pH: 6.0.

(a) Separation of 0.48-mM α-chy, 0.88-mM cyt C in 3.72 column volumes; (b) simulation.

train. Figure 3 represents a feed volume slightly greater than the maximum feed volume that can be completely separated under these chromatographic conditions. As noted above, it is a substantial loading of the column, and this separation results in the purification of a large amount of protein.

Figures 4a and 4b present a comparison of simulated and experimental displacements for the conditions described for Figure 1d. The feed load is 5.3 times the maximum isotachic feed load. As noted earlier, loading was continued past the column saturation point, resulting in a combination of multicomponent frontal and nondeveloped displacement. As seen in the figure, excellent agreement between theory and experiment is observed. Again, the displacer breakthrough is well predicted (approximately 6.3 column volumes). The cytochrome C zone has formed a relatively small square zone at the rear of the train with a concentration of approximately 1.1 mM. Ahead of this developed zone, the cytochrome C band spikes up to a concentration of approximately 3.5 mM. In fact, the nondevelopment spike of cytochrome C could be visually monitored as a dark brown band moving down the column within a light brown band. At the beginning of this zone, a second region of constant concentration (approximately 0.9 mM) was observed. The rear of the α-chymotrypsinogen band contains a spike of approximately 1.4 mM. Prior to that two constant concentration zones of 0.3 mM (right zone) and 1.0 mM (left zone) emerge. This is an important result in that it indicates the model can indeed be used for describing multicomponent equilibria under nonlinear conditions.

The significance of the results presented in Figures 2 through 4 is dramatic. Using a relatively simple set of data [k' vs. salt concentration data at infinite dilution and a nonlinear concentrated peak or front (Gadam et al., 1993; Gallant et al., 1994)] it is possible to predict the displacement of protein separations using the SMA-based model. In the next section, the utility of this chromatographic model will be examined by further comparison of theory and experiment.

Comparison of experiment and theory under other salt conditions

Although induced salt gradients in displacement chromatography cause substantial deviations of the actual microenvironment salt concentrations from the "carrier" salt concentration, the concentration of salt introduced at the column inlet plays an important role in control and optimization of the displacement process. Having established the reliability of the model at 75-mM salt concentration, it was desir-

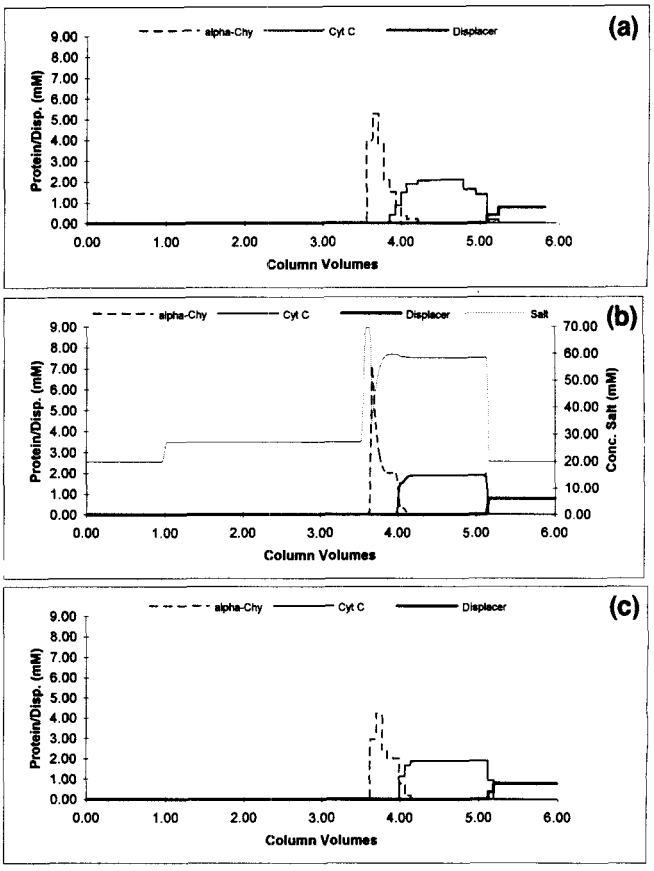

Figure 5. Transient displacement of α-chymotrypsinogen and cytochrome C by 0.78-mM 40 kD DEAE dextran in 20-mM sodium phosphate at pH: 6.0.

(a) Separation of 0.44-mM α-chy, 0.83-mM cyt C in 2.55 column volumes; (b) simulation; (c) simulated 100-μL fraction collection carried out on simulation depicted in b.

able to explore the validity of model predictions across a range of carrier salt concentrations. A value of 20 mM was selected as the "low" carrier salt concentration, because at this concentration the microenvironment salt concentrations will be determined to a large extent by the induced salt gradients. A value of 97 mM was chosen as the "high" carrier salt concentration, because significantly higher concentrations would result in elution rather than displacement of the proteins, a potentially undesirable side effect of induced salt gradients.

Figure 5 shows a displacement separation of α-chymotrypsinogen and cytochrome C conducted at 20-mM carrier salt concentration. A feed volume of 2.55 column volumes (3.5 mL) of 0.44-mM α-chymotrypsinogen and 0.83-mM cytochrome C was loaded during the feed cycle. As seen in the figure, even at such high feed loading (78 mg total protein), almost complete separation of the two components was achieved. Furthermore, good agreement between theory and experiment was observed. Comparing the experimental result (Figure 5a) to the simulation (Figure 5b), the displacer has broken through at the expected point (approximately 5.2 column volumes). In both figures, the cytochrome C forms an almost completely isotachic band of concentration 1.9 mM with a small region of nondevelopment at the front of the zone. The α-chymotrypsinogen exists in a small region of incomplete separation and in a highly concentrated spike that rises up to approximately 7.0 mM in the simulation and 5.0 mM in the experiment. This overprediction of the α-chymotrypsinogen concentration can be understood based on the fraction collection protocol employed in the experimental procedure. The simulation (Figure 5b) depicts a smooth continuous profile. When the simulation is replotted accounting for this 100 μL fraction collection (Figure 5c), the sharp spike in α-chymotrypsinogen concentration is no longer so obvious. At the same time the front of displacer has become somewhat more disperse in appearance. The effects of the fraction collection and analysis should certainly be considered as the reader examines the experimental and theoretical results presented in this article. However, simulated fraction collection has not been employed throughout this article because it results in a loss of information.

Comparison of Figure 5 (20-mM salt in the carrier) and Figure 3 (75-mM salt in the carrier) indicate that similar levels of nondevelopment are present in the two displacements. However, in the 20-mM separation, the protein loading was 50% higher. This suggests that displacement development proceeds more rapidly at lower salt concentrations, resulting in increased productivity. The isotachic concentrations are also higher at lower salt conditions, resulting in a more pronounced concentration effect during the displacement process.

Examination of the simulated chromatogram (Figure 5b) reveals that approximately 40 mM of the 60-mM salt concentration in the protein zones was induced by the displacer. The existence of such large induced salt gradients has been documented in previous work (Brooks and Cramer, 1992; Jayaraman et al., 1993; Gerstner and Cramer, 1992a,b). Since the choice of displacer has a large effect on the magnitude of these induced salt gradients, careful consideration should be given to the SMA parameters of potential displacer molecules. This subject is addressed elsewhere in a systematic treatment by Brooks and Cramer (1994).

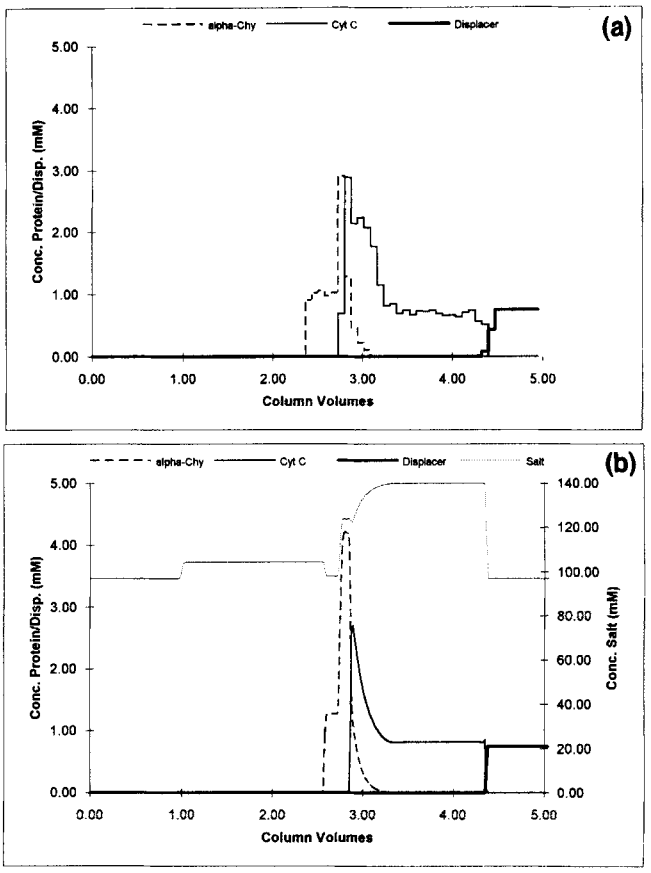

Figure 6. Transient displacement of α-chymotrypsinogen and cytochrome C by 0.75-mM 40 kD DEAE dextran in 97-mM sodium phosphate at pH: 6.0.

(a) Separation of 0.48-mM α-chy, 0.86-mM cyt C in 1.75 column volumes; (b) simulation.

In Figure 6, a displacement experiment at 97 mM carrier salt with a feed volume of 1.75 column volumes of 0.48-mM α-chymotrypsinogen and 0.86-mM cytochrome C is presented. This is the same feed load employed in the experiment depicted in Figure 3. In both the experimental chromatogram (Figure 6a) and the simulation (Figure 6b), the cytochrome C forms a square zone of concentration 0.7 mM at the end of the displacement train. Further forward in the train, the cytochrome C spikes up to approximately 3.0 mM just prior to 3.0 column volumes. The α-chymotrypsinogen exists in a small mixed zone at the beginning of the cytochrome C. Immediately ahead of that, the cytochrome C spikes up sharply and, at the front of the train, forms a constant concentration zone of approximately 1.2 mM.

The displacements depicted in Figures 6 and 3 were carried out with the same feed load and with carrier salt concentrations of 97 and 75 mM, respectively. The displacement carried out at 75-mM carrier salt resulted in essentially complete separation of the proteins. In contrast, the displacement carried out at 97 mM had a more pronounced mixed region, indicating that the increase in carrier salt resulted in less development of the displacement process. This result, in concert with the result presented in Figure 5, indicates that it is indeed desirable to operate at lower carrier salt conditions.

Conclusions

The theoretical and experimental results presented in this article indicate that the SMA-based model is indeed well suited for simulating nondevelopment in protein displacement systems. Having observed the behavior of displacement development over a range of operating conditions, a number of observations may be made with regard to the productivity of displacement separations. First, operation under conditions of incomplete development offers a way to increase the productivity of a given displacement separation. Particularly when a relatively high affinity protein (which will arrange itself at the rear of the displacement train) is the object of purification, it will be possible to load substantially more than the isotachic feed load while still satisfying rigorous standards of purity and yield.

The second observation from this work is that, for the same feed load, displacement development proceeds much faster at lower salt concentration. Thus, reduction of the carrier salt concentration offers a means to boost the separation productivity. One *caveat* with respect to this point is that as the salt microenvironment of the protein bands decreases in magnitude, the kinetics of desorption may adversely affect the separation. It has been observed that the displacement boundaries can become less sharp at extremely low salt concentrations.

Clearly, the optimization of the production rate in displacement chromatography will most likely involve nondeveloped scenarios. The SMA-based model is currently being employed in concert with rigorous optimization techniques to study the optimization of both displacement and nonlinear gradient systems and will be the subject of a future report.

Acknowledgments

This research was funded by Millipore Corporation and a Presidential Young Investigator Award to S. M. Cramer from the National Science Foundation.

Notation

C_i = mobile phase concentration, mM
$C_{i,f}$ = feed concentration, mM
D_i = effective diffusion coefficient, cm^2/s
F_i = function which returns Q_i when given C_1, C_2,...C_{NC}, mM
H = height equivalent to a theoretical plate, cm
K_{1i} = equilibrium constant
L = column length, cm
N = theoretical plates per meter, m^{-1}
NC = number of components present in mobile phase
Q_i = stationary phase concentration, mM
$Q_{i,max}$ = maximum possible single-component bound protein concentration, mM
$\bar{Q}_1$ = bound salt which is not sterically shielded, mM
$\hat{Q}_1$ = bound salt which is sterically shielded, mM
t = time dimension, s
u_0 = chromatographic velocity, $u_0 = u_s/\epsilon$, cm/s
Z = axial dimension of column, cm

Greek letters

ϵ = void fraction
Λ = column capacity, mM
ν_i = characteristic charge
σ_i = steric factor

Subscript

i = mobile/stationary phase component number ($i = 1$ designates salt)

Literature Cited

Antia, F. D., and C. Horváth, "Analysis of Isotachic Patterns in Displacement Chromatography," *J. Chromatog.*, **556**, 119 (1991).
Berninger, J. A., R. D. Whitley, X. Zhang, and N. H. L. Whang, "A Versatile Model for Simulation of Reaction and Nonequilibrium Dynamics in Multicomponent Fixed-Bed Adsorption Processes," *Comput. Chem. Eng.*, **15**, 749 (1991).
Brooks, C. A., and S. M. Cramer, "Steric Mass-Action Ion-Exchange: Displacement Profiles and Induced Salt Gradients," *AIChE J.*, **38**, 1969 (1992).
Brooks, C. A., and S. M. Cramer, "Solute Affinity in Ion-Exchange Displacement Chromatography," *Chem. Eng. Sci.*, in press (1995).
Cramer, S., and G. Subramanian, "Recent Advances in Theory and Practice of Displacement Chromatography," *Sep. Purif. Methods*, **19**, 31 (1990).
Czok, M., and G. Guiochon, "The Physical Sense of Simulation Models of Liquid Chromatography: Propagation Through a Grid or Solution of the Mass Balance Equations," *Anal. Chem.*, **62**, 189 (1990).
De Bokx, P. K., P. C. Baarslag, and H. P. Urbach, "Modeling of Displacement Chromatography Using Nonideal Isotherms," *J. Chromatog.*, **594**, 9 (1992).
Felinger, A., and G. Guiochon, "Comparison of Maximum Production Rates and Optimum Operating/Design Parameters in Overloaded Elution and Displacement Chromatography," *Biotechnol. Bioeng.*, **41**, 134 (1993).
Frenz, J., and C. Horváth, "High Performance Displacement Chromatography: Calculation and Experimental Verification of Zone Development," *AIChE J.*, **31**, 400 (1985).
Frenz, J., and C. Horváth, "High Performance Displacement Chromatography," *High Performance Liquid Chromatography — Advances and Perspectives*, Vol. 8, C. Horváth, Academic Press, Orlando, FL (1988).
Gadam, S. D., G. Jayaraman, and S. M. Cramer, "Characterization of Non-Linear Adsorption Properties of Dextran-Based Polyelectrolyte Displacers in Ion-Exchange Systems," *J. Chromatog.*, **630**, 37 (1993).
Gadam, S. D., and S. M. Cramer, "Pentosan Polysulfate as a Non-Toxic Low Molecular Weight Displaced Chromatography," *Chromatographia*, **39**, 409 (1994).
Gallant, S. G., A. Kundu, and S. M. Cramer, "Modeling Non-Linear Elution of Proteins in Ion-Exchange Chromatography," *J. Chromatog.*, in press (1995).
Gerstner, J. A., and S. M. Cramer, "Cation-Exchange Displacement Chromatography of Proteins with Protamine Displacers," *Biotechnol. Prog.*, **8**, 540 (1992a).
Gerstner, J. A., and S. M. Cramer, "Heparin as a Non-Toxic Displacer for Anion Exchange Displacement Chromatography of Proteins," *BioPharm*, **5**, 42 (1992b).
Ghose, S., and B. Mattiasson, "Evaluation of Displacement Chromatography for the Recovery of Lactate Dehydrogenase From Beef Heart Under Scale-Up Conditions," *J. Chromatog.*, **547**, 145 (1991).
Gu, T., G. Tsai, and M. R. Ladisch, "Displacement Effect in Multicomponent Chromatography," *AIChE J.*, **36**, 1156 (1990).
Helfferich, F. G., and G. Klein, *Multicomponent Chromatography*, Marcel Dekker, New York (1970).
Helfferich, F., and P. Carr, "Non-Linear Waves in Chromatography: I. Waves, Shocks, and Shapes," *J. Chromatog.*, **629**, 97 (1993).
Horváth, C., "Displacement Chromatography: Yesterday, Today, and Tomorrow," in *The Science of Chromatography*, F. Bruner, ed., Elsevier, Amsterdam (1985).
Jayaraman, G., S. D. Gadam, and S. M. Cramer, "Ion-Exchange Displacement Chromatography of Proteins: Dextran-Based Polyelectrolytes as High-Affinity Displacers," *J. Chromatog.*, **630**, 53 (1993).
Jen, S. C. D., and N. G. Pinto, "Dextran Sulfate as a Displacer for the Displacement Chromatography of Pharmaceutical Proteins," *J. Chromatog. Sci.*, **29**, 1 (1991).
Jen, S. C. D., and N. G. Pinto, "Theory of Optimization of Ideal

Displacement Chromatography of Binary Mixtures," *J. Chromatog.*, **590**, 3 (1992).
Knox, J. H., and H. M. Pyper, "Framework for Maximizing Throughput in Preparative Liquid Chromatography," *J. Chromatog.*, **363**, 1 (1986).
Liao, A., Z. El Rassi, D. LeMaster, and C. Horváth, "High Performance Displacement Chromatography of Proteins: Separation of β-Lactoglobulins A and B," *Chromatographia*, **24**, 881 (1987).
Ma, Z., and G. Guiochon, "Applications of Orthogonal Collocation on Finite Elements in the Simulation of Non-Linear Chromatography," *Comput. Chem. Eng.*, **15**, 415 (1991).
Myers, A. L., "Activity Coefficients of Mixtures Adsorbed on Heterogeneous Surfaces," *AIChE J.*, **29**, 691 (1983).
Peterson, E., and A. Torres, "Ion-Exchange Displacement Chromatography of Serum Proteins, Using Narrow Range Carboxymethyl Dextrans and a New Index of Affinity," *Anal. Biochem.*, **130**, 271 (1983).
Phillips, M. W., G. Subramanian, and S. M. Cramer, "Theoretical Optimization of Operating Parameters in Nonideal Displacement Chromatography," *J. Chromatog.*, **454**, 1 (1988).
Rhee, H. K., R. Aris, and N. R. Amundson, "On the Theory of Multicomponent Chromatography," *Phil. Trans. Roy. Soc. Lond. A*, **267**, 419 (1970).
Rhee, H. K., R. Aris, and N. R. Amundson, *First-Order Partial Differential Equations: II*, Prentice-Hall, Englewood Cliffs, NJ (1989).
Velayudhan, A., "Studies in Nonlinear Chromatography," PhD Dissertation, Yale University (1990).
Wankat, P. C., *Rate-Controlled Separations*, Elsevier, London (1990).
Yu, Q., T. S. Nguyen, and D. D. Do, "Interference Phenomena and Non-Ideal Effects of Displacement Chromatography," *Preparative Chromatog.*, **235**, 1 (1991).

Manuscript received June 3, 1994, and revision received Sept. 15, 1994.